

$$= \frac{e^{iR\varphi}}{F(e^{i\varphi})} \sum_{r=0}^{R-1} \left( \sum_{m=0}^{R-1-r} a_m e^{-i(m+r)\varphi} \right) \sum_{\nu=1}^{\sigma} T_r^{(\nu)}$$

$$\therefore \sum_{\nu=1}^{\sigma} D_{\nu}'(\varphi) = \frac{\sum_{n=0}^{R-1} \left( \sum_{m=0}^n a_m T_{n-m} \right) e^{-in\varphi}}{\sum_{n=0}^R a_n e^{-in\varphi}} \quad (88)$$

which is equivalent to equations (35) and (45).

### References

- ALLEGRA, G. (1961). *Acta Cryst.* **14**, 535.  
 ALLEGRA, G. (1964). *Acta Cryst.* **17**, 579.  
 GEVERS, R. (1952). *Acta Cryst.* **5**, 518.  
 GEVERS, R. (1954a). *Acta Cryst.* **7**, 337.  
 GEVERS, R. (1954b). *Acta Cryst.* **7**, 492.  
 HENDRICKS, S. & TELLER, E. (1942). *J. Chem. Phys.* **10**, 147.  
 JAGODZINSKI, H. (1949a). *Acta Cryst.* **2**, 201.  
 JAGODZINSKI, H. (1949b). *Acta Cryst.* **2**, 208.  
 JAGODZINSKI, H. (1949c). *Acta Cryst.* **2**, 298.  
 JAGODZINSKI, H. (1954). *Acta Cryst.* **7**, 17.  
 KAKINOKI, J. & KOMURA, Y. (1952). *J. Phys. Soc. Japan*, **7**, 30.  
 KAKINOKI, J. & KOMURA, Y. (1954a). *J. Phys. Soc. Japan*, **9**, 169.  
 KAKINOKI, J. & KOMURA, Y. (1954b). *J. Phys. Soc. Japan*, **9**, 177.  
 KAKINOKI, J. & KOMURA, Y. (1962). *Acta Cryst.* **15**, 292.  
 KOMURA, Y. (1962). *Acta Cryst.* **15**, 770.  
 MÉRING, J. (1949). *Acta Cryst.* **2**, 371.  
 PATERSON, M. S. (1952). *J. Appl. Phys.* **23**, 805.  
 WARREN, B. E. & WAREKOIS, E. P. (1955). *Acta Metallurg.* **3**, 473.  
 WARREN, B. E. (1959). *Prog. Met. Phys.* **8**, 147.  
 WILSON, A. J. C. (1942). *Proc. Roy. Soc., A*, **180**, 277.  
 WILSON, A. J. C. (1943). *Proc. Roy. Soc., A*, **181**, 360.  
 ZACHARIASEN, W. H. (1947). *Phys. Rev.* **71**, 715.

## Short Communications

Contributions intended for publication under this heading should be expressly so marked; they should not exceed about 1000 words; they should be forwarded in the usual way to the appropriate Co-editor; they will be published as speedily as possible. Publication will be quicker if the contributions are without illustrations.

*Acta Cryst.* (1965). **19**, 147

**Antiferromagnetism in nickel orthosilicate\***. By R. NEWNHAM, R. SANTORO, J. FANG† and S. NOMURA‡, *Electrical Engineering Dept., Massachusetts Institute of Technology, Cambridge, Massachusetts, U.S.A.*

(Received 24 November 1964)

Nickel orthosilicate,  $\text{Ni}_2\text{SiO}_4$ , is isomorphous with the mineral olivine. Polycrystalline specimens were prepared from sodium orthosilicate and nickel nitrate. After the components were dissolved separately in distilled water, the orthosilicate solution was slowly added to the nitrate solution, yielding a hydrated nickel silicate precipitate. The precipitate was filtered and washed, and then fired at  $1400^\circ\text{C}$  for 24 hours to give  $\text{Ni}_2\text{SiO}_4$ . Least-squares refinement of high-angle X-ray diffractometer data gave the lattice parameters  $a = 10.121 \pm 0.005$ ,  $b = 5.915 \pm 0.002$ ,  $c = 4.727 \pm 0.002$  Å. The space group is  $Pnma$  with four formula-units per unit cell.

A vibrating-sample magnetometer was used to measure the magnetic susceptibility of  $\text{Ni}_2\text{SiO}_4$ . As shown in Fig. 1, the susceptibility follows a Curie-Weiss law above  $60^\circ\text{K}$ , with  $\theta = 7^\circ\text{K}$  and  $p_{\text{eff}} = 3.15 \mu_B$ . Kondo & Miyahara (1963) report slightly different values of  $-14^\circ\text{K}$  and  $3.04 \mu_B$ . The susceptibility goes through a maximum near  $34^\circ\text{K}$ , indicative of a paramagnetic-antiferromagnetic transition.

\* Sponsored by Advanced Research Projects Agency under contract SD-90 and by the U.S. Air Force under Contract AF33(616)-8353.

† Present address: Geology Department, Southern Illinois University, Carbondale, Illinois, U.S.A.

‡ Present address: Physics Department, Tokyo Institute of Technology, Ookayama, Meguro-ku, Tokyo, Japan.

Neutron diffraction patterns of polycrystalline  $\text{Ni}_2\text{SiO}_4$  taken above and below the Néel temperature are shown in Fig. 2. The nuclear intensities (Table 1) agree well with values calculated from the olivine coordinates (Hanke & Zemann, 1963), confirming the crystal structure. The magnetic peaks in the low-temperature pattern cannot be in-

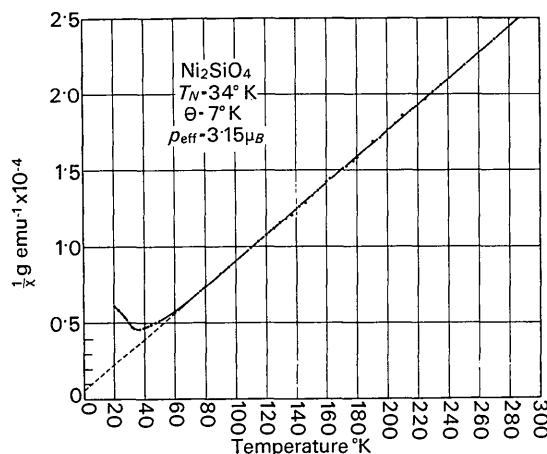


Fig. 1. The reciprocal susceptibility of  $\text{Ni}_2\text{SiO}_4$  plotted as a function of temperature.

Table 1. Comparison of observed and calculated nuclear intensities indexed on the chemical unit cell.

$hkl$	$d_{\text{calc}}$	$I_{\text{calc}}$	$I_{\text{obs}}$	$d_{\text{obs}}$
200	5.06	3	2	5.08
101	4.28	4	6	4.29
210	3.85	5	4	3.86
011	3.69	3	3	3.71
111	3.47	25	30	3.48
201	3.45	2		
211	2.98	2	4	2.98
020	2.96	2		
301	2.75	35	30	2.76
220	2.55	4	6	2.56
400	2.53	2		
311	2.49	22	26	2.49
121	2.43	39	36	2.44

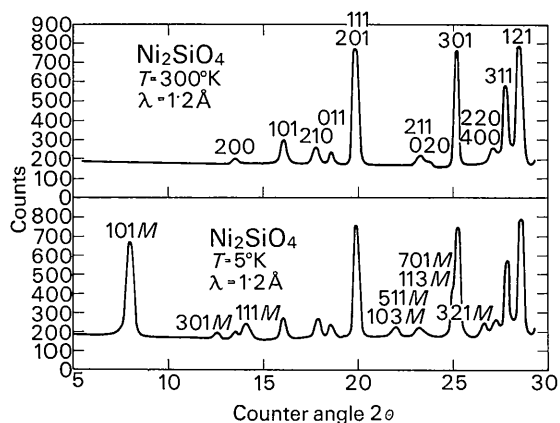


Fig. 2. Neutron diffraction powder patterns of  $\text{Ni}_2\text{SiO}_4$  taken above and below the antiferromagnetic transition. Indices for the nuclear intensities are given in the room-temperature pattern. The magnetic reflections ( $M$ ) in the low-temperature pattern are indexed on an orthorhombic magnetic cell with dimensions  $20.2 \times 5.9 \times 9.5 \text{ \AA}$ .

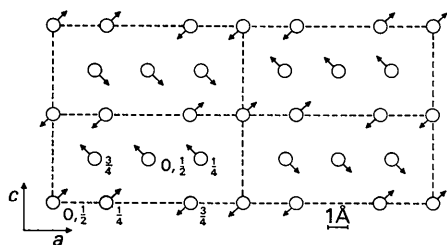


Fig. 3. Possible spin arrangement in antiferromagnetic  $\text{Ni}_2\text{SiO}_4$  projected on (010). Heights of the Ni ions are expressed in cell fractions; silicon and oxygen positions are not shown. The magnetic superlattice and four chemical sub-cells are outlined.

dexed on the chemical unit cell and require a  $2a \times b \times 2c$  superlattice cell containing 32 nickel atoms. This many spin directions cannot be established with certainty from the powder diagram, but the antiferromagnetic alignment in Fig. 3 gives reasonable agreement with experiment (Table 2). The computational methods outlined by Shirane (1959) proved useful in calculating the magnetic intensities.

Table 2. Comparison of observed and calculated magnetic intensities indexed on the magnetic superlattice

$hkl$	$d_{\text{calc}}$	$I_{\text{calc}}$	$I_{\text{obs}}$	$d_{\text{obs}}$
101	8.57	33	36	8.60
301	5.51	1	3	5.49
111	4.87	6	7	4.88
311	4.03	1	<2	—
501	3.72	1	<2	—
511	3.15	2	3	3.14
103	3.12	2		
303	2.86	0	<2	—
121	2.80	0	<2	—
701	2.77	2	2	2.77
113	2.76	1		
321	2.60	6	5	2.60
711	2.51	0	<2	—

The model was derived from the magnetic structure of cobalt orthosilicate (Nomura, Santoro, Fang & Newnham, 1964), in which spins at height  $z=0$  in the chemical cell are antiparallel to those at  $z=\frac{1}{2}$ . The cobalt moments are collinear with  $\mathbf{b}$ . When indexed on the quadrupled cell, the magnetic reflections of  $\text{Ni}_2\text{SiO}_4$  are absent unless  $h$  and  $l$  are odd, suggesting that spins related by translational vectors along  $\mathbf{a}$  and  $\mathbf{c}$  are antiparallel. Intensity calculations were carried out for a number of four-spin models similar to the  $\text{Co}_2\text{SiO}_4$  arrangement and consistent with the  $B$ -face centering condition. The best results were achieved with the spins in (010), as indicated in Fig. 3. Within this plane only relative spin directions can be determined from the powder pattern; rotation of the entire spin system about  $\mathbf{b}$  yields identical intensities.

We wish to acknowledge our indebtedness to Prof. C. G. Shull, Mr M. J. Redman, and the staff of the M.I.T. Computation Center.

#### References

- HANKE, K. & ZEMANN, J. (1963). *Naturwissenschaften*, **50**, 91.  
 KONDO, H. & MIYAHARA, S. (1963). *J. Phys. Soc. Japan*, **18**, 305.  
 NOMURA, S., SANTORO, R., FANG, J. & NEWNHAM, R. (1964). *Phys. Chem. Solids*, **25**, 901.  
 SHIRANE, G. (1959). *Acta Cryst.* **12**, 282.